South East France Potentially Active Faults:
A database for seismic hazard assessment

Victoria Mowbray[1], Christian Sue[1], Stephane Baize[2], Céline Beauval[1], Marguerite Mathey[2], Anne Lemoine[3], Andrea Walpersdorf[1], Eloïse Granier[1]

[1]Institut Sciences de la Terre, UGA, USMB, CNRS, IRD, OSUG, Gières, France
[2]Autorité de Sûreté Nucléaire et de Radioprotection, Fontenay-aux-Roses, France
[3]Bureau de Recherches Géologiques et Minières, Orléans, France

Correspondence to: Victoria Mowbray (victoria.mowbray@univ-grenoble-alpes.fr)

Abstract. The South-East of France has been structured by numerous tectonic episodes resulting in a complex compound of crustal deformations. This fallouts in a large network of faults which have evolved throughout subsequent tectonic events. Nevertheless, the present-day tectonic deformation is slow and of debated origin, giving place to a low to moderate seismicity. This seismotectonic context is a challenge for seismic hazard analysis, specifically for the identification and characterisation of potentially active faults. In this study we present a fault-related data compilation, named South-East France Potentially Active Faults (SEFPAF, Mowbray et al., 2025, https://doi.org/10.5281/zenodo.17235395), which integrates structural components from geological maps, previous neotectonic databases and fault-specific studies. Our objective is to provide a new, well documented, and modular fault database. Multiple structural representations per fault are presented, allowing the end-user to choose from the various parameter value options. With an end purpose of identifying the most relevant faults for seismic hazard assessment, we build a series of indices which allow fault prioritization: the Importance index (I), the Documentation index (D) and, the Seismogenic Potential index (SP). The first classifies faults into major, secondary and minor based on the source's description of the structure; the second analyses the quantity of information known for each fault; the last intends to decipher seismically active faults by integrating the age of the last documented rupture, the spatial correlation with seismic flux and, the spatial correlation with geodetic strain. SEFPAF may have various applications, amongst them we illustrate the first step towards the development of a fault model for seismic hazard analysis: we identify relevant faults to model by adjusting the index criteria and, propose idealized geometries for a set of 20 faults which can subsequently be used as composite seismogenic sources.

Summary. We present a fault-related data compilation, named South-East France Potentially Active Faults (SEFPAF). It integrates structural components and presents a fault classification by importance, amount of documentation and seismogenic potential. This last parameter is assessed by analysing the amount of observed seismicity near the faults, amount of surface deformation estimated from GNSS velocities, and the age of the last known rupture on the fault.

1 Introduction

35 The South-East of France encompasses a complex geological structure shaped by a multi-phase tectonic history. The region retains basement faults from the Variscan Orogeny, typically NE-SW oriented (Arthaud and Matte, 1975; Matte and Burg, 1981; Matte and Mattauer, 1987). These reactivated during post-Variscan phases accommodating the gravitational collapse of the belt (Ménard and Molnar, 1988; Malavieille et al., 1990; Malavieille, 1993), the forming of the Tethyan margin (Mohn et al., 2012), and the Pyrenean–Alpine Orogeny (e.g. Boudon et al., 1976; Handy et al., 2010; Manatschal et al., 2022). During

40 the Alpine convergence, new structures are also formed: E–W oriented in the Provence-Pyrenean domain and wrapping the Apulo-Adriatic indenter in the Western Alps (e.g. Tapponnier, 1977; Gratier et al., 1989; Bellahsen et al., 2014; Angrand and Mouthereau, 2021). This episode spans from the Eocene to the early Pliocene, experiencing an extensional phase during the Oligo-Miocene, which shaped the French South-East basin (e.g. Roure et al., 1992; Le Pichon and Rangin, 2010). This extended tectonic history results in a high variety and density of fault systems comprising all deformation modes, the current

45 activity of which is still under debate.

The current seismicity is contrasted amongst the high-chain of the Western Alps (with focal mechanisms in extension and transtension) and its peripheral areas and basins (strike-slip and transpression) (Sue et al., 1999; Delacou et al., 2004, 2005; Mathey et al., 2021), consistent with GNSS datasets (Walpersdorf et al., 2015, 2018). Additionally, field studies recognise normal faulting since the Miocene in the internal zones of the belt (e;g. Bistacchi and Massironi, 2000; Champagnac et al.,

50 2003; Sue and Tricart, 2003; Bertrand and Sue, 2017; Bilau et al., 2021). Seismic rates are low to moderate (no earthquakes Mw > 6.0 recorded during the instrumental period, Larroque et al., 2022; Fig. 1) and the crustal deformation is slow (< 20 nanostrain, Walpersdorf et al., 2018; Masson et al., 2019; Serpelloni et al., 2022). Nevertheless, about 10 Mw 5 and 1 Mw 6 events have been recorded per century since 1300 AD within the considered region (Fig. 1; Manchuel et al., 2018; BCSF-Rénass, 2022), pointing to a significant activity. Furthermore, paleoseismic studies on specific faults suggest that surface

55 rupturing earthquakes with magnitude larger than Mw 6.5 have occurred in the region within the Holocene, with an estimated minimum recurrence time of 10 ky (Sébrier et al., 1997; Bellier et al., 2022). It is thus crucial for seismic hazard assessments (SHA) to study the faults capable of accommodating such earthquakes. Given the seismotectonic context and, the relatively short time windows of seismic records and GPS data acquisition, the geophysical identification of active faults is a challenging task. Furthermore, paleo-seismic investigations are hindered by the fast erosional processes in the region (Sébrier et al., 1997;

60 Valla et al., 2021) which erase most of the geomorphic evidence of tectonic activity.

Active faults are structures capable of releasing seismic energy in the near future. Their identification criteria is disputed in the literature (Slemmons and McKinney, 1977; Muir Wood and Mallard, 1992; Machette, 2000; Wu and Hu, 2024). In this study, we consider a fault as potentially active when it meets one or various of the following criteria: it is located near significant observed seismicity; it lies within an area undergoing above-average crustal deformation (> 5 nanostrains); there is

65 evidence of Quaternary activity. The latter criteria is recommended by the international nuclear safety guideline (IAEA, 2010) as well as by other authors (Machette, 2000; Wu and Hu, 2024) who emphasize the need to consider multiple long-term seismic

cycles (> 10 ky). Moreover, we are interested in faults capable of producing Mw 5.5 or above. After scaling laws, such event requires a rupture plane of a minimum length of about 5 km (Leonard, 2014).

This work provides a new open-access, easy to use and modular fault catalogue named SEFPAF (South-East France Potentially
70   Active Faults, Mowbray et al., 2025, https://doi.org/10.5281/zenodo.17235395) which aims to identify and characterize important, documented and potentially seismogenic faults. Previous efforts toward a fault database for SHA of metropolitan France have been made (Jomard et al., 2017), yet their work is concentrated in the vicinities of nuclear sites (< 50 km). Our compilation intends to continue this work, with a regional focus, by integrating updated information on known structures. We opt for an extended geographical coverage in order to include fault data that can contribute to the seismic hazard in south-east
75   France in a consistent manner (Fig. 1). To do so, we combine and sort structural data from the literature and geological maps, as well as introduce a criteria-driven approach to discriminate faults relevant for seismic hazard amongst the synthetized database.

At last, SEFPAF can contribute to the characterisation of seismic source models for SHA as an input for fault-based models or seismotectonic zonation models. We illustrate the initial phase of developing such a model by characterising a set of critical
80   faults for earthquake recurrence modeling, based on an index-driven pre-selection of faults from SEFPAF.

2 Data

To build SEFPAF we select and compile fault data from geological maps, former neotectonic fault datasets, regional fault mapping and, neotectonic evidences (see Table 1). We integrate the following datasets:

85   1) Geological maps (Fig. 2a)

We start by resembling the structural lines from the 1/1 000 000 scale geological maps of France (Chantraine et al., 2003), Italy (Pantaloni, 2021) and Switzerland (swisstopo, 2024). While all three datasets provide high resolution, densely-mapped surface fault traces, they only rarely present further information. The French geological map offers occasional information on the name of the fault, kinematics, dip direction, and fault importance. From this map we integrate 1819 fault segments. The
90   Italian map provides information on the kinematics, dip direction, fault importance and reliability of the trace when known. The Swiss map offers occasional information on fault names, kinematics, fault importance and reliability of the trace. We integrate 216 fault segments from the Italian map and 30 fault segments from the Swiss map.

2) Neotectonic fault datasets (Fig. 2b)

95   We include previous efforts of characterising potentially active faults in France. Yet each database is built with a different purpose and with a different geographical extention.

(i) We firstly consider the "BDFA" (Base de Données de Failles Actives) from Jomard et al. (2017), which aims to map active faults in the 50 km vicinity of nuclear facilities within metropolitan France. They focus on characterising faults capable of

producing Mw > 6 events, thus including faults with a minimum length of 10 km. It represents the most detailed compilation
100 of potentially active faults in France at present, incorporating a comprehensive assemblage of paleo-seismic studies. The
surface fault traces are based on the work of Grellet et al. (1993) and Terrier (2004), improved with the use of geological maps,
digital elevation models, aerial photographs and specific publications. They also integrate the faulting evidences from Baize
et al. (2002) and NEOPAL (Bertrand et al., 2007, data accessible at https://data.oreme.org/fact/fact_map). When available, the
dataset provides the following information for each fault segment: geometry, extension in depth, kinematics, age of last known
105 rupture, field observations, paleoseismic slip rates (decomposed into vertical and horizontal components), and geodetical slip
rates. It presents 136 faults for metropolitan France, of which we integrate 76 in our SEFPAF compilation, represented as 173
segments.

(ii) We integrate the "PACA-PO" (Provence, Alpes, Côte d'Azur et Pyrenees Orientales) fault dataset (Terrier et al., 2018),
produced with the aim to identify potentially active faults over the realm of Eastern Pyrenees, Rhône Valley and Provence.
110 Their work is focused on the methodological development of identifying active faults, yet it provides, as an example, a
potentially active fault database. Their mapping draws from earlier sources including Terrier (1991), Ritz (1991), Blès et al.
(1992), and French geological maps at scales 1/250 000 and 1/ 50 000 (Janjou, 2004). It integrates seismotectonic, seismic and
geodetic data from extensive published literature. It is mapped at scale 1/250 000 and provides attributes such as fault name,
the age of the last known rupture and the kinematics. We integrate all of the 178 fault segments it comprises.

115 (iii) We then incorporate the neotectonic fault map from Grellet et al. (1993). As this dataset served as a foundational source
for the BDFA Jomard et al. (2017), we only integrate the fault segments which are not already included, to avoid redundancy.
Its mapping is based on a vast structural literature and integrates fault information from the available geophysical and
paleoseismic data at the time. Its fault traces occasionally contrast the geological map and it presents a simplified cartography.
It informs on the age of the last known rupture, the kinematics, the fault importance and the reliability of the trace. From this
120 source we integrate the 203 fault segments within our study zone.

(iv) For the Italian part of our target area, we include the ITHACA (Italian HAzard from CApable faults) dataset in the Po
plain and the Ligurian sea (Comerci et al., 2013). It summarizes the available information on faults that are expressed at the
surface, affecting the Italian territory with evidence of activity within the last 40 ky. This database is managed by the
Geological Survey of Italy (SGI), initiated in 2000 (Michetti et al., 2000) and it is constantly being updated (data accessible at
125 https://sgi.isprambiente.it/ithaca/viewer/index.html). It provides data on the kinematics of the fault, the age of last known
rupture and the reliability on the trace. We integrate 150 fault segments from this dataset.

3) Regional studies (Fig. 2c)

We include specific fault studies in order to provide more detailed fault traces. In that way, the High Durance fault system is
based on the morphotectonic and fieldwork surveys from Sue and Tricart, (2003). The Vuache fault is extended towards the
130 north with the mapping from Lallemand et al. (2024). The Belledonne fault system is based on the seismotectonic analysis
from Thouvenot et al., (2003), extended east with the Arcalod fault and west with the Brion fault (Billant et al., 2015). The

northern extension of the Cevennes fault system - notably La Rouvière fault - is incorporated from Thomasset et al. (2024). The active fault representation of the southern Alps is included (Sanchez et al., 2010), as well as other studies for the regions of Aosta, Valais and Ligure (Bistacchi and Massironi, 2000; Champagnac et al., 2003; Morelli et al., 2022). Fault traces have also been gathered from the studies of seismic swarms such as the Ubaye swarm (Jenatton et al., 2007) and the Maurienne swarm (Guéguen et al., 2022), which propose fault planes responsible of the episodes by using high precision event relocation methods.

4) Neotectonic evidences (Fig. 2c)

We also integrate neotectonic evidences from the NEOPAL database (Bertrand et al., 2007) and from ASNR indexes (Baize et al., 2002). Both are inventories of paleo-seismic, tectonic and geomorphic evidences of fault displacement within the Quaternary. NEOPAL is a national database updated and maintained until 2009, while the ASNR database was published in 2002. Both provide information on field observations, fault kinematics, reliability of the evidence and, the neotectonic age of the last activity. From NEOPAL, we integrate 37 evidences within the study zone which present a strong or very strong confidence, while from ASNR, all the 60 evidences within the zone are included.

3 Methodology

A leading objective of this work is to integrate all the data without redundancy while preserving the key information from each dataset. Different datasets occasionally provide conflicting information for the same faults, offering varying surface traces and characteristics. To address this issue, we establish a hierarchical order for the input datasets, namely: Regional studies > Potentially Active faults databases > Neotectonic evidences > structural lines from geological maps. This sequence guides the selection of faults for cartographic representation, while retaining the multiple attribute data in the inventory. Additionally, we standardize the parameter and value terminology amongst all source datasets in order to harmonize the database vocabulary.

In the SEFPAF database, each row is referred to as an *entity,* which can be a fault segment or a neotectonic evidence. Multiple entities can correspond to the same fault. There are 2649 entities for a total of 1729 faults.

To build the actual SEFPAF database, we follow these 6 steps:

Step 1) The structural lines are sorted, by excluding low angle alpine nappe contacts and faults with a length of less than 5 km. Low angle thrusts require large strain rates to re-activate, which is inconsistent with the low compression rates in the region. A minimum fault length of ~5 km is required to generate an earthquake with magnitude larger or equal to Mw 5.5 (Leonard, 2014, interplate dip slip scaling relationship).

Step 2) The faults from all datasets are grouped by fault systems based on spatial distribution, fault orientation, and tectonic domain (Fig. 3). This classification provides a structured framework that helps the end user correlate geological structures and offers a tectonic perspective for subsequent fault-specific studies.

Step 3) Merging of the datasets is then applied by fault system, in order to facilitate the visual analysis of overlapping segments which could belong to one same fault.

165 Step 4) Segments from different sources which represent the same fault are then identified and assigned a unique fault ID, consolidating all information from different datasets under a single identity. The hierarchical rank is then applied in order to select a unique fault trace for the mapping of SEFPAF (example in Fig. 4).

Step 5) Neotectonic evidences within 2 km of a fault are incorporated to the catalog as entities linked to that fault's ID.

Step 6) To achieve the SEFPAF database, we gather the following parameters for every entity: fid, ID, Fault System, Fault ID,

170 Fault name, Neotectonic Evidence name, Neotectonic Evidence observations, Source, Trace representation, Trace coordinates, Importance, Reliability, Neotectonic age, Strike, Dip, Dip Direction, Length, Depth, Kinematics, Slip. See section *SEFPAF structure* for further information.

Once the fault catalog is composed, we apply a methodology to sort and prioritize faults. In this purpose, indexes are developed for the *importance*, *documentation*, and *seismogenic potential* of faults in order to establish quantitative classification criteria

175 for SEFPAF.

3.1 Importance index (I, Fig. 5a)

This index classifies the structures as minor (1), secondary (2) and major (3), after the information given in the input datasets. This value is subsequently weighted according to the hierarchical order (Regional studies > Potentially Active faults databases

180 > Neotectonic evidences > structural lines from geological maps). For the cases where fault importance is not specified in the input data, only the source ranking applies, resulting in an automatic classification. For example, structures coming from regional studies are designated as major faults by default, as these studies generally focus on structures with significant geological importance.

3.2 Documentation index (D, Fig. 5b)

185 This index reflects the quantity of information available for a given fault. For each fault, we quantify the parameters for which we have information, across all entities belonging to the same structure. With a total of 10 fault parameters in SEFPAF ('Fault name', 'Reliability', 'Importance', 'Strike', 'Kinematics', 'Slip', 'Dip', 'Direction', 'Depth', 'Neotectonic age'), we consider a fault as undocumented (D = 0) when only one or no parameters are known, poorly documented (D = 1) when 2 to 4 parameters are

190 known, moderately documented (D = 2) when 5 to 7 parameters are known, and, well documented (D = 3) when 8 to 10 parameters are known.

3.3 Seismogenic Potential index (SP, Fig. 5c)

We intend to evaluate the potential seismic activity of a fault after three criteria; age of neotectonic activity, near fault

195 seismicity, and near fault geodetic strain. For this we generate a set of sub-indexes which are subsequently integrated in the Seismogenic Potential index (SP).

3.3.1 Neotectonic sub-index (Fig. 6a)

A value ranging from -1 to 5 is assigned after the documented last activity of the fault. This information in SEFPAF
is rare and, it corresponds to paleoseismic or historical data. Non documented activity corresponds to a value of -1 in
the database, Pre-Miocene activity, to a value 0, Miocene activity, 1, Pliocene activity, 2, Pleistocene activity, 3,
Holocene activity, 4, and historical activity, 5 (Fig. 6a).

3.3.2 Near fault seismicity sub-index (Fig. 6b, 6c)

In order to take into account the seismicity in relation to the faults, we assess the seismic flux spatial distribution from
earthquake data (BCSF-Rénass catalog for the instrumental period, (1962 - 2021, BCSF-Rénass, 2022) and FCAT
for the early instrumental and historical period (462 - 1962, Manchuel et al., 2018)). We analyse the seismicity on a
grid of hexagonal cells of 0.1 ° (11 km) of diameter (Fig. 6b), thus allowing for uncertainties on seismic events and
fault location. We compute the seismic moment from each event using the equation $M_0 = 10^{(1.5Mw + 9.1)}$ [N·m] from
Hanks and Kanamori (1979). Within each cell, the total seismic moment rate is calculated from all earthquakes falling
inside the cell, accounting for time windows of completeness (Table 2). We then categorize logarithmically the
seismic flux into eight moment rate classes (Fig. 6b). SEFPAF faults are thereafter assigned a score from 1 to 8
corresponding to the highest seismic flux cell they intersect, giving place to the near fault seismicity sub-index (Fig.
6c).

3.3.3 Near fault geodetic deformation sub-index (Fig. 6d, 6e)

Next, we analyze the amplitude of surface deformation using GNSS strain solutions (Piña-Valdés et al., 2022 -
interpolated data every 0.1 ° - 11 km - using VISR software (Shen et al., 2015)) in order to take into account the
available geodetic data in the SP index. We examine the point data within rectangular cells (0.1 ° x 0.1 °) filling the
entirety of the study zone. We consider the amplitude of the strain as $E = \max (|e_{min}|, |e_{max}|, |e_{min} + e_{max}|)$ (Masson et
al., 2019), and categorize it in 5 levels; < 3 nanostrain, 3 - 5 nanostrain, 5 - 7 nanostrain, 7 - 9 nanostrain, > 9 nanostrain
(Fig. 6d). Similarly to the near fault seismicity sub-index, we assign a score (1 – 5) after the intersection of the faults
with the highest strain category cell (Fig. 6e).

With the aim to integrate these three sub-indexes into the SP index, we normalize them to a 0–100 scale, making them
numerically comparable. A weighted average is computed by assigning arbitrary weights: 0.25 to the neotectonic subindex,
0.5 to the near-fault seismicity sub-index, and 0.25 to the near-fault deformation sub-index. This ponderation reflects the
relative confidence in each data- type. The neotectonic sub-index gives direct evidence of a major event occurring on the fault
within the Quaternary, thus confirming the activity of the fault. So far, this information is heterogeneously available throughout
SEFPAF and is therefore considered partial. The near-fault seismicity sub-index offers the most recent and direct evidence for

seismic activity. Both the neotectonic and near fault seismicity sub-indexes imply an inductive reasoning, drawing conclusions on seismic potential based on patterns from past earthquake data. In contrast, the deformation sub-index doesn't rely on past

230 seismic observations, but instead, on a model of crustal deformation which is subject to uncertainties in GNSS-derived strain solutions and eventual aseismic processes. Each of these methods presents its limitations; we assign a higher weight to the near fault seismicity sub-index due to its direct information on seismic activity.

The I, D and SP indexes allow for the classification of SEFPAF, in which there are 2649 entities for a total of 1729 faults. From these, only 10% are identified as major faults (I = 3), 37% have a documentation index greater than 0, and less than 20%

235 have a seismogenic potential index above 30 (Fig. 7). The distributions of the individual seismogenic potential sub-indices are represented in Figure 8. The neotectonic sub-index reveals that only ~ 15% of the SEFPAF faults have a documented rupture age, with 8% corresponding to Quaternary ages. The near-fault seismicity sub-index reflects that roughly 10% of the faults lie within an area of released seismic flux higher than 1.7×10^{13} N·m/y (including the 4 upper seismic moment bins). The near-fault deformation sub-index shows that about 10% of the faults intersect regions of geodetic strain of > 5 nanostrain.

4 SEFPAF database structure

240

The purpose of this study is to develop a new, well-documented and modular fault database. To achieve this, we incorporate all the available information from the various source datasets presented in the *Data* section. As a result, a single fault may have several representations with differing parameter values (Fig. 4). By keeping the complete original information in the database, end users are able to critically evaluate and select the most appropriate information, according to their criteria.

245 The parameters we provide in SEFPAF are the following:

4.1 Fid, ID,   Fault_System,   Fault_ID

These parameters allow for data identification and organisation. The *fid* value is unique for each entity, ranging from 1 to 2649. Entities are grouped under the same fault ID based on their geological continuity, spatial proximity and shared characteristics. Faults are grouped by systems (Fig. 3, namely: Aosta Ranzola, Belledonne - Pelvoux, Central Sub-Alpine Front, Cevennes,

250 Forez, Insubrian line, Jura, Ligure, Ligurian Alps, Massif-Central, Middle Durance, Eastern Pyrenees, Penninic Front, Pilat, Po, Provence, Rhine, Rhône line, Salon-Cavaillon - Ventoux, Southern Alps, Western Sub-Alpine Front) in order to reflect similar geometries, tectonic history and potential behavior. This classification may support further analyses on potential combined ruptures and fault mechanisms. *Fault_ID* is a unique numeric identifier per fault within the fault system, ranging from 1 to n faults in the system. We assign each fault a unique identifier (*ID*) by concatenating Fault_System and Fault_ID.

255

4.2 Fault_name, NE_name, NE_observations

Some entities include the name of the fault (*Fault_name*) or the name of the neotectonic evidence (*NE_name*). The latter comprises a numeric code and location as specified in their source database (Baize et al., 2002; Bertrand et al., 2007). We add a parameter for the documented observations of the neotectonic evidences (*NE_observations*).

260 ### 4.3 Source

Here we indicate the source dataset reference from where the entity information originates: Geological map of France, Geological map of Switzerland, Geological map of Italy, Terrier et al., 2018, Jomard et al., 2017, Grellet et al., 1993, Comerci et al., 2013, Thouvenot et al., 2003, Sue et Tricart, 2003, Jenatton et al., 2007, Gueguen et al., 2022, Sanchez et al., 2010, Champagnac et al., 2003, Bistacchi et Massironi, 2000, Morelli et al., 2022, Billant et al., 2015, Lallemand, et al., 2024,
265 Thomasset et al., 2024.

4.4 Trace_rep, WKT, WKT_on_map

One fault may be described by multiple entities, offering different information, as well as variations in the surface fault trace. However, only one fault trace is displayed on the SEFPAF map. Whether the trace is represented cartographically or not is indicated in the parameter *Trace_rep* with the respective values 1 or 0, for true or false. *WKT* is the Well-Known Text
270 geometrical representation in coordinates in the EPSG:4326 - WGS 84 coordinate system. WKT is preserved for each entity; it is a linestring or multilinestring for fault segments, and a point coordinate for neotectonic evidences. *WKT_on_map* is the column of *WKT* for entities where *Trace_rep* is 1, representing the geometries to be reflected on the SEFPAF fault map.

4.5 Importance, Reliability, NeoT_age

This group of parameters reflects raw fault values representing the fault importance, the reliability of the information, location,
275 or existence of the fault, and the neotectonic age of the last rupture. *Importance* is expressed in values of 1, 2, 3, for minor, secondary and major fault. *Reliability* is expressed in values from 0 to 1, reflecting uncertain to certain. *NeoT_age* is expressed in text for the geological periods, series, ages or glacial-interglacial phases.

4.6 Strike, Dip, DipDir, Length, Depth

280 These parameters describe the main geometrical characteristics of the faults. *Strike* is the angle of main orientation of the fault trace in relation to the North, expressed in º. *Dip* is the angle of dipping of the fault plane in relation to the horizontal, also expressed in º. *DipDir* informs of which direction the fault dips, expressed in N, E, S, W, and their potential combinations. *Length* and *Depth* give the dimensions of the fault plane in km. The length is computed after the WKT geometry while the

285 depth comes from the source dataset when known or assumed. This information is infrequently specified in the input datasets, it is primarily documented in Jomard et al. (2017) and some regional studies.

4.7 Kinematics, Slip

Here we reassemble the information on the fault's kinematics and the slip rate when documented in the input data. The *Kinematics* determines the last fault's mechanics as normal (N) or reverse (R) in the perpendicular axis followed by the parallel movement, after '/', and expressed as strike-slip (SS) -left-lateral (S) or -right-lateral (D), when oblique. This parameter is 290 present in most datasets but not for all entities. The *Slip* is the displacement rate on the fault in mm/y, calculated from geological offsets, available for few entities originating from Jomard et al. (2017) and some regional studies (Billant et al., 2015; Lallemand et al., 2024). These slip rates are gathered in the database but are not used for index criteria, given the heterogeneous nature of this information across SEFPAF.

4.8 I, D, SP_n, SP_s, SP_d, SP

295 These are the indexes and sub-indexes we generate for fault classification. *I* is the importance index assigned to each fault, retaining the highest importance value among its entities. This index is expressed as 1, 2, 3 referring to minor, secondary and major faults. *D* reflects how well a fault is documented based on the completeness of parameter values (fault name, strike, dip, dip direction, depth, kinematics, slip rate, neotectonic age, reliability, importance) across entities of one same fault ID. Values range from 0 (least) to 3 (most documented). *SP_n, SP_s, SP_d* are the Seismogenic Potential sub-indexes, corresponding to 300 the neotectonic sub-index, the near fault seismicity sub-index, and the near fault geodetic deformation sub-index. The first ranges from -1 to 5, the second from 0 to 8 and the third from 1 to 5. *SP* is the Seismogenic Potential index expressed in values from 0 to 100; it incorporates the 3 previous sub-indexes weighted by 0.25, 0.5 and 0.25 respectively.

5 Potential Applications

The SEFPAF (South-East France Potentially Active Faults) database offers a diverse range of possible applications across 305 multiple geophysical and geological disciplines. It can serve for instance as a foundational resource for local or regional structural geology analysis. In seismotectonics it can enhance the comprehension of seismic processes by allowing correlations amongst structural and seismic data. For geodynamic and mechanical studies, SEFPAF offers information on the upper crust structure, contributing to insights into regional tectonic behaviour. Additionally, this database can be valorized in seismic hazard assessments, acting as an input for establishing seismotectonic zonation models or building fault-based seismogenic 310 source models.

Indeed, our primary goal to build SEFPAF database is to characterise seismic sources for seismic hazard in South-East France. After Haller and Basili (2011) a seismogenic source is a generalized, three-dimensional representation of a dipping surface in the earth's crust where fault slip occurs and where most of the seismic energy is released during an earthquake. In order to

model a seismogenic source it is necessary to assume an idealized geometry and a constant slip rate that best reflexes reality,
315   thus, only faults presenting a minimum set of assets can be included. Specifically, we require the coordinates of the fault trace,
the extension at depth, dip angle and direction, slip rate and a predetermined maximum magnitude that the fault may host in
the future.

Based on these requirements, we sort the most important, well-documented, and potentially seismogenic faults from the
SEFPAF database by using the following selection criteria: Importance index > 1, Documentation index > 0 and Seismogenic
320   Potential index > 22. A total of 230 faults are nominated (Fig. 9a). We reduce this assemblage into a more synthetic structural
map encompassing 20 faults (Fig. 9b), each represented as a single trace, by selecting the main structure within compound
fault systems while prioritising those with significant studies and substantial geodetic data (for a subsequent estimate of on-
fault deformation). The modeled faults (Table 3) retain the dominant geometric trends, the highest index values, and the
youngest evidence of neotectonic rupture, derived from the multiple SEFPAF entities describing the fault.

325   Our choice to adopt a simple and reduced set of faults to include in a fault model is driven by the interest to provide robust
geodetic slip rate estimations - limited by GNSS data availability – given the general lack of geological slip rates in the region.
Given the current structural and geodetic knowledge of the region, we consider that modeling earthquake recurrence using a
single representative fault trace—rather than multiple segment traces—is presently the most appropriate approach. This doesn't
disregard fault segmentation, rather, using long faults we account for multi-segment ruptures, as implemented e.g. in DISS
330   (Basili et al., 2008; DISS Working Group, 2021). This approach follows the concept of *composite seismogenic sources* (Basili
et al., 2008), where an idealized fault geometry is defined, yet the maximum magnitude is independent from the structure
dimensions - allowing for a large range of potential ruptures within the fault bounded by predefined minimum and maximum
magnitudes. Moreover, this approach is in line with the general geological understanding that faults are often complex and
segmented at surface but may root and simplify at depth (Ben-Zion and Sammis, 2003; Share et al., 2020).

335   **6 Data availability**

The South-East France Potentially Active Faults (SEFPAF) dataset can be downloaded from ZENODO website:
https://zenodo.org/records/17235395 with the following DOI: https://doi.org/10.5281/zenodo.17235395 (Mowbray et al.,
2025). In the repository the following files are collected:

- *SEFPAF.csv* contains all fault data as entities (different fault information from each input source).
340   - *SEFPAF.html* is the data presented in a user friendly mapview.
- *SEFPAF_compilation_code.ipynb* is the python code used to compile and analyse all the input data.
- *INPUT.zip* contains all the input files used in the python code as csv files.

Citation:

Mowbray, V., Sue, C., Baize, S., Beauval, C., Mathey, M., Lemoine, A., Walpersdorf, A., & Granier, E.: South East France
345   Potentially Active Faults [Data set]. Zenodo. https://doi.org/10.5281/zenodo.17235395, 2025

Earth System
Science
Data

7 Conclusions

The South East of France Potentially Active Faults (SEFPAF) database is a fault data compilation which integrates relevant structural, kinematic and neotectonic information from previous fault related studies. It is a modular database which includes data from different sources even when non-consistent. It interprets and translates the combined information into one standard
350   format. Further on, we propose a unique representation of surface trace per fault when various representations exist amongst sources. Subsequently, we design and apply classification indexes to each fault which allow to determine the level of importance, of documentation and of seismogenic potential. This classification allows to select faults from the database by customizing the index criteria.

We identify various scientific applications for the SEFPAF database. These underscore the value of the here presented fault
355   catalog towards advancing geological and geophysical research for the South-East of France, specifically targeting seismic hazard studies. We illustrate the first step towards building a fault-based source model for seismic hazard assessment by making a selection of important, well characterised and potentially seismogenic faults.

We acknowledge the limitations of this fault compilation, which stem from the continuously evolving data – such as new structural interpretations, paleoseismic studies, and new seismic and geodetic acquisitions. Additionally, the logic of our three
360   indexes of selection carries inherent assumptions: the *Importance index* is mainly based on input data, which varies depending on the criteria and interpretations defined by the authors in each source; the *Documentation index* reflects the amount of information per fault, assessing the quantity and not intrinsically the quality of the data; the *Seismogenic Potential index* is constructed on a set of hypothesis and requires weighting of sub-indices – rising questions such as whether the observed seismicity is a more reliable indicator of future seismic activity, than GNSS-derived strain or neotectonic evidence. We
365   therefore encourage users to make use of this dataset with an understanding of its underlying assumptions and limitations.

9 Author contribution

VM produced the data compilation, wrote the code for compiling, selected manually which segments and evidences belonged to one same fault ID, and designated the fault system classification. Moreover, VM proposed the indexes for fault prioritisation, produced the figures and wrote the core of the paper. CS and SB contributed by suggesting regional studies to include as well
370   as bringing a tectonic perspective into the fault system classification. CB brought expertise in seismic hazard and seismic flux computation, by adjusting the completeness periods of the seismic catalogs. MM, AL and AW suggested methods to analyse faults with geodesy and seismicity for fault indexing. EG contributed by facilitating a user-friendly map file to view the data. All coauthors revised the paper.

10 Competing interests

The authors declare that they have no conflict of interest.

11 Acknowledgements

This work was financially supported by the PEPR IRiMa project - PC NaTech (https://www.pepr-risques.fr/fr/risques-natech-anticiper-gerer-accidents-technologiques-engendres-par-un-evenement-naturel-dans, ANR-22-EXIR-0006) from the French Ministry of Regional planning and Ecological transition, and by the RGF Alpes project (https://rgf.brgm.fr/page/alpes-bassins-peripheriques) from the Bureau de Recherches Géologiques et Minières (BRGM) of France.

385
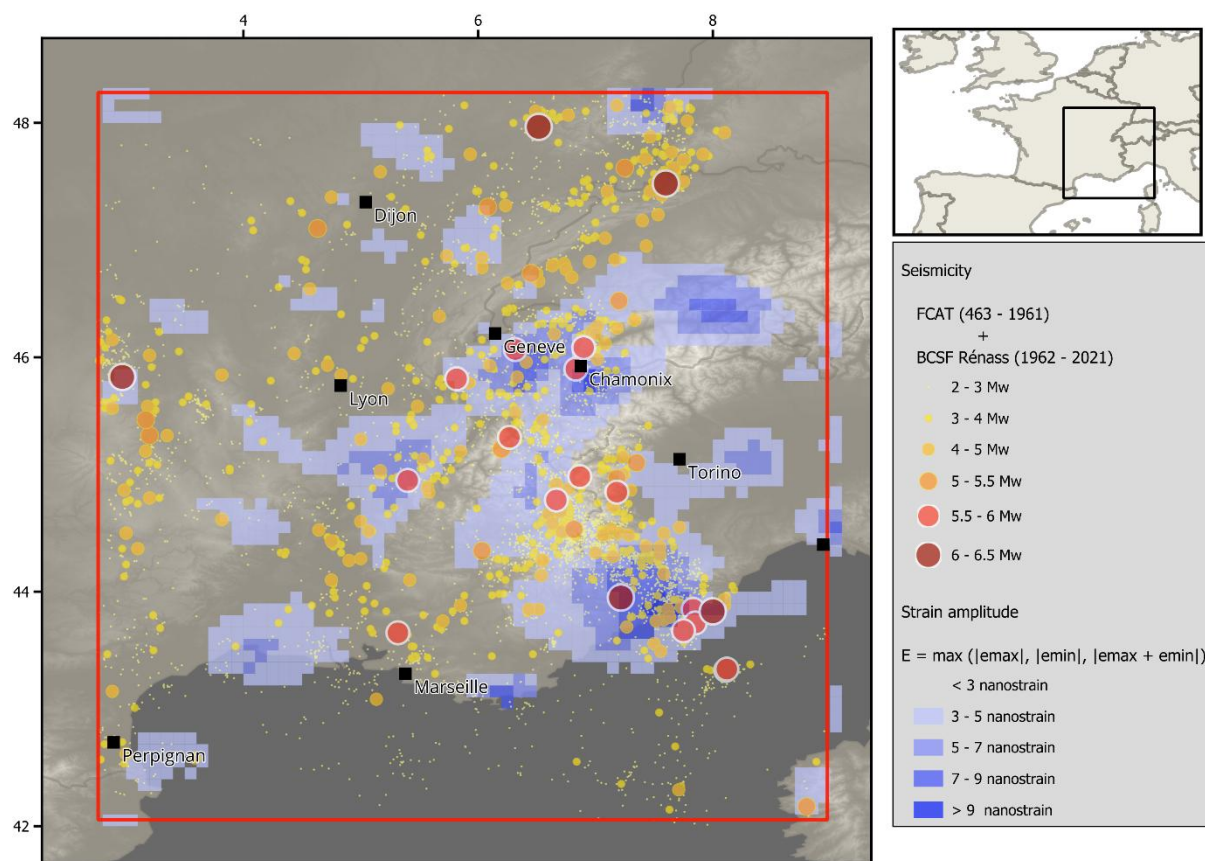
Figure 1

Past seismicity and geodetic strain estimate within the studied region (red rectangle). FCAT earthquake catalog (Manchuel et al., 2018) for the period 463 to 1961 and the BCSF Rénass catalog (BCSF-Rénass, 2022) for the instrumental period 1962-2021. The surface strain amplitude is represented in shades of blue after 5 strain bins (strain values from Piña-Valdès et al.,
390   2022).
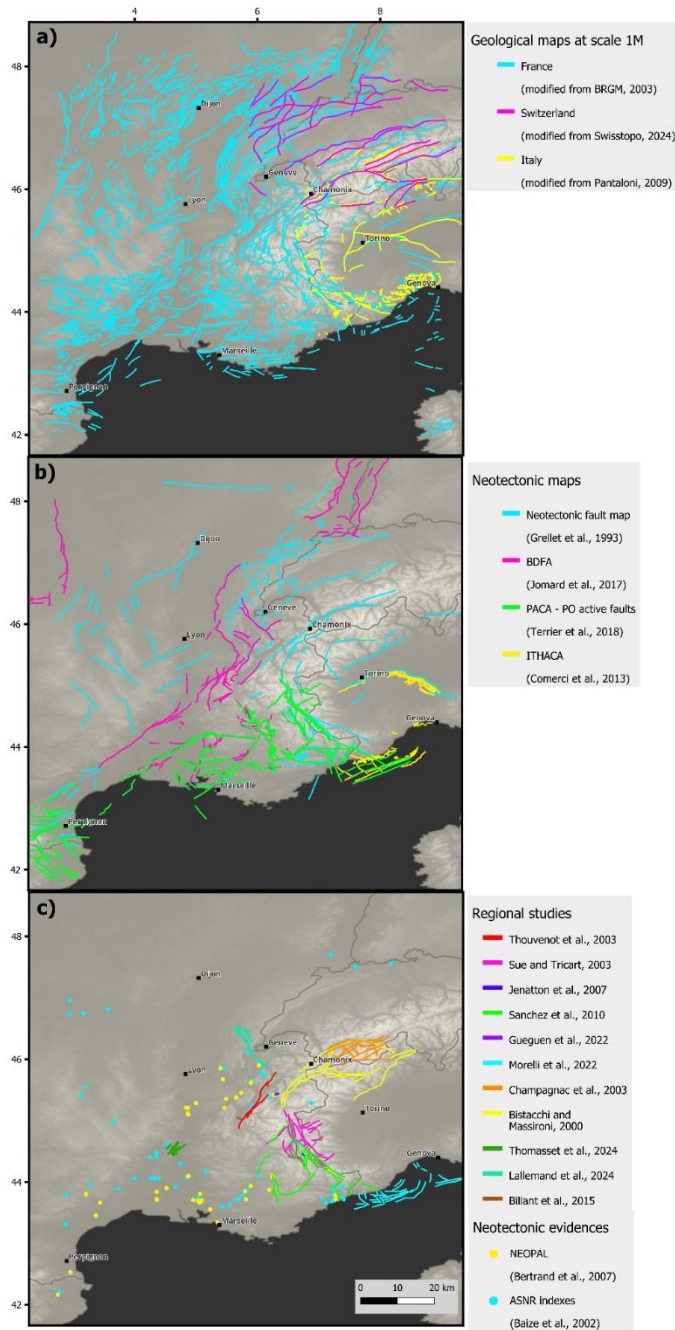
Figure 2

Input datasets for the SEFPAF compilation. A) Fault traces from geological maps; B) Fault traces from neotectonic maps; C) Fault traces from regional studies and neotectonic evidences.

395
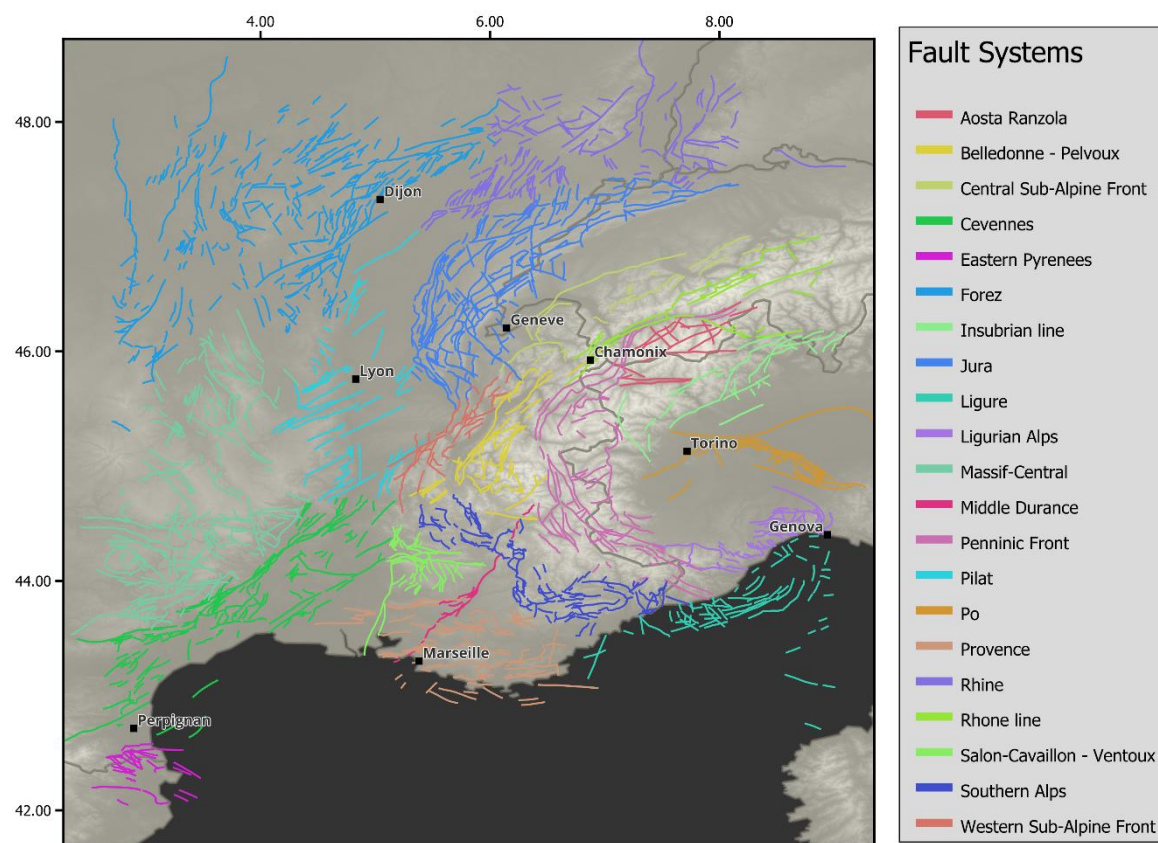
Figure 3

The SEFPAF map showing the fault system classification. Here one single, unique fault trace per fault is mapped, avoiding the multiple cartographical representation of one fault – often caused by multiple data sources - by selecting the most reliable

400   fault representation based after the imposed hierarchal order (see Methodology) that reflects the considered data source reliability.
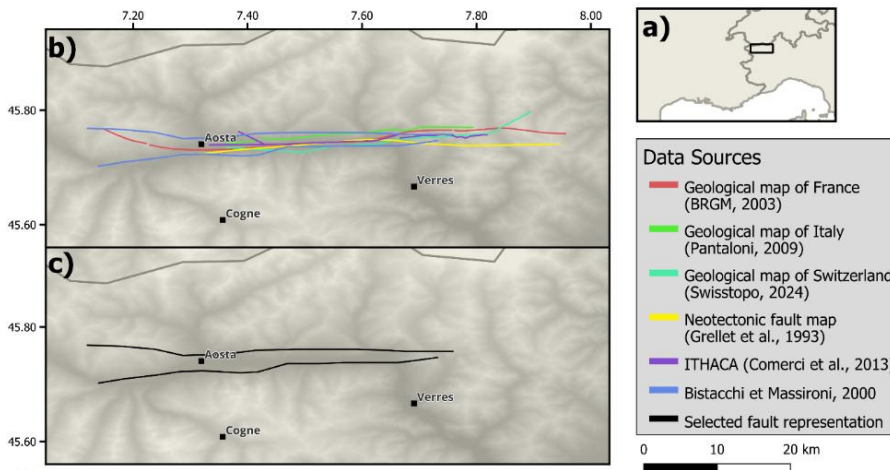
Figure 4

405 Example of the Aosta-Ranzola fault with multiple representations. All available source data are preserved as separate entities within the SEFPAF database, but only one representation is selected for display on the fault map—here, the trace from Bistacchi and Massironi (2000). A) Overview map showing the location of panels b and c. B) All fault trace representations in SEFPAF identified as the Aosta-Ranzola fault. Despite differing geometries and segmentations, these are interpreted as the same fault. C) The selected fault for display on the SEFPAF map according to the hierarchical reliability ranking of source

410 data.
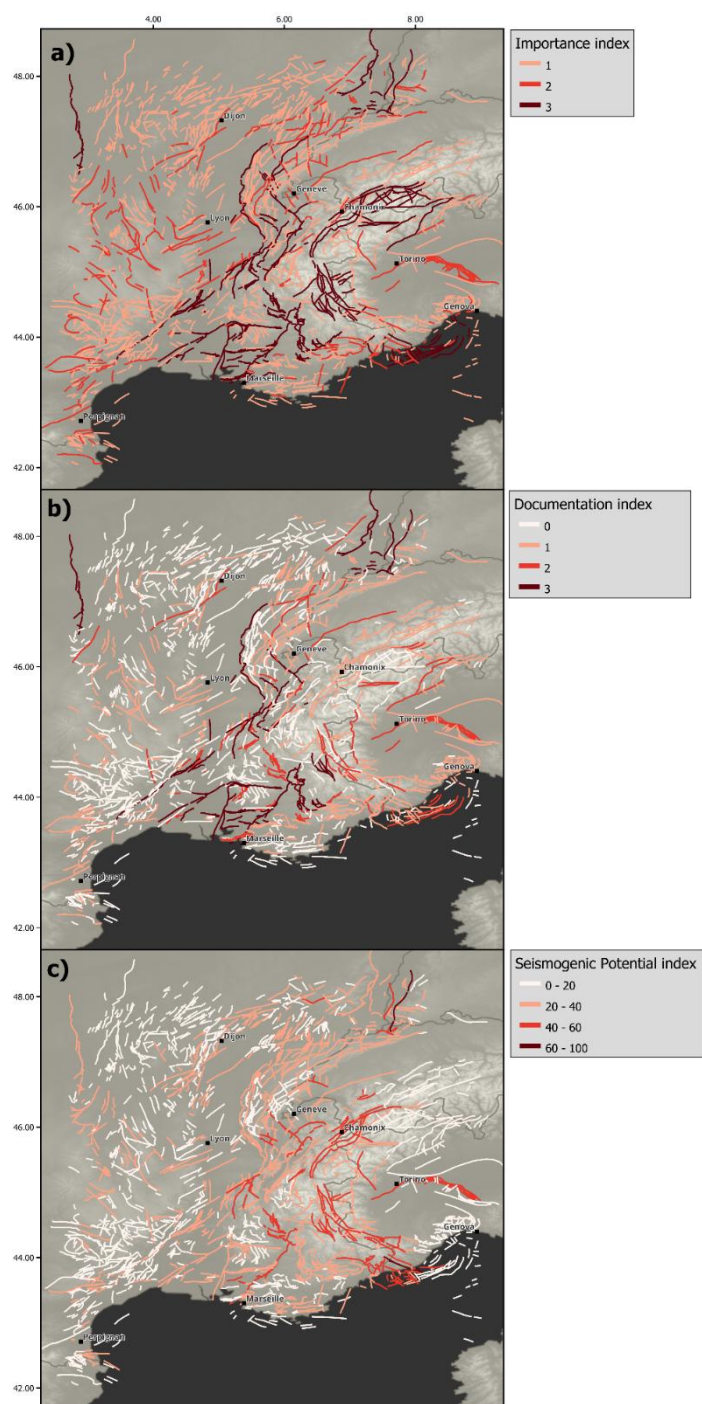
Figure 5

Classification indices. A) Importance index; B) Documentation index; C) Seismogenic Potential index.
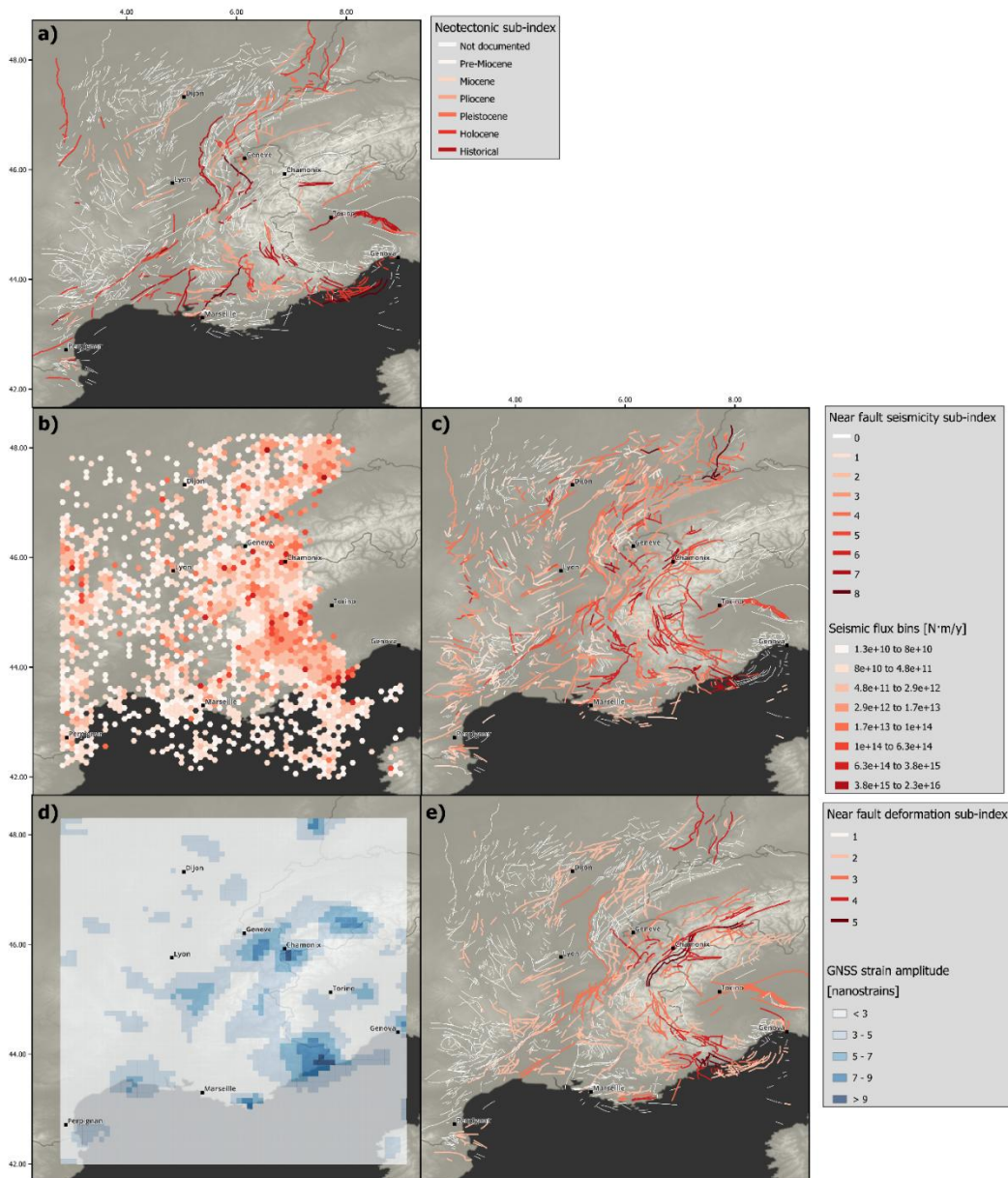
Figure 6

Seismogenic Potential sub-indices; A) Neotectonic sub-index; B) Seismic flux distribution computed from the seismic catalogs FCAT (Manchuel et al., 2018) + BCSF Rénass (BCSF-Rénass, 2022) ; C) Near fault seismicity sub-index; D) GNSS strain amplitude modified from Piña Valdès et al. (2022); E) Near fault deformation sub-index.
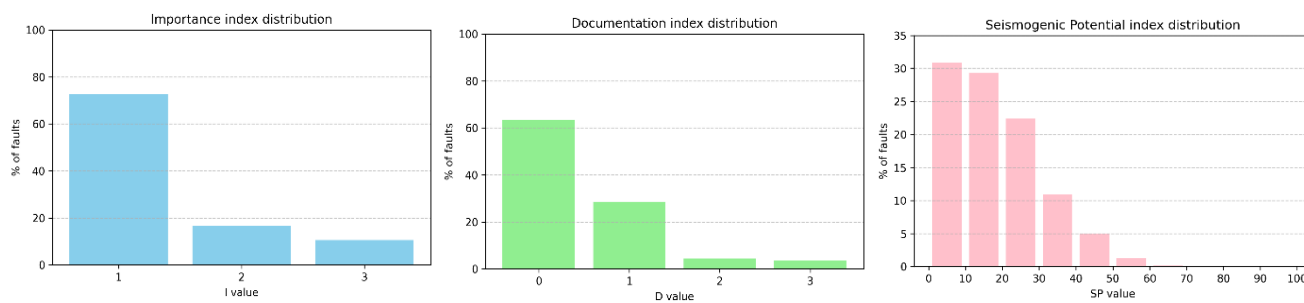
420 **Figure 7**

Distribution of the percentage of faults in SEFPAF for the indices Importance, Documentation and Seismogenic Potential.
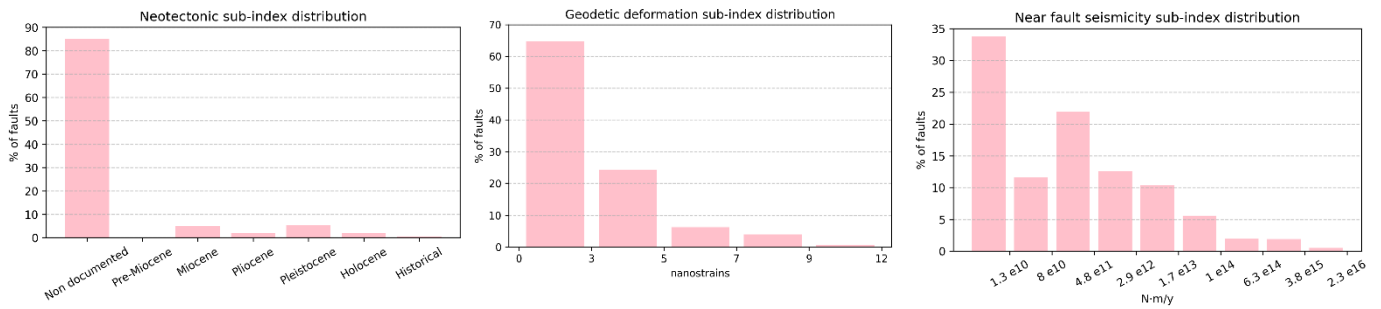
Figure 8

425   Distribution of the percentage of faults in SEFPAF for the sub-indices: Neotectonic, Near-fault geodetic deformation and Near-fault seismicity.
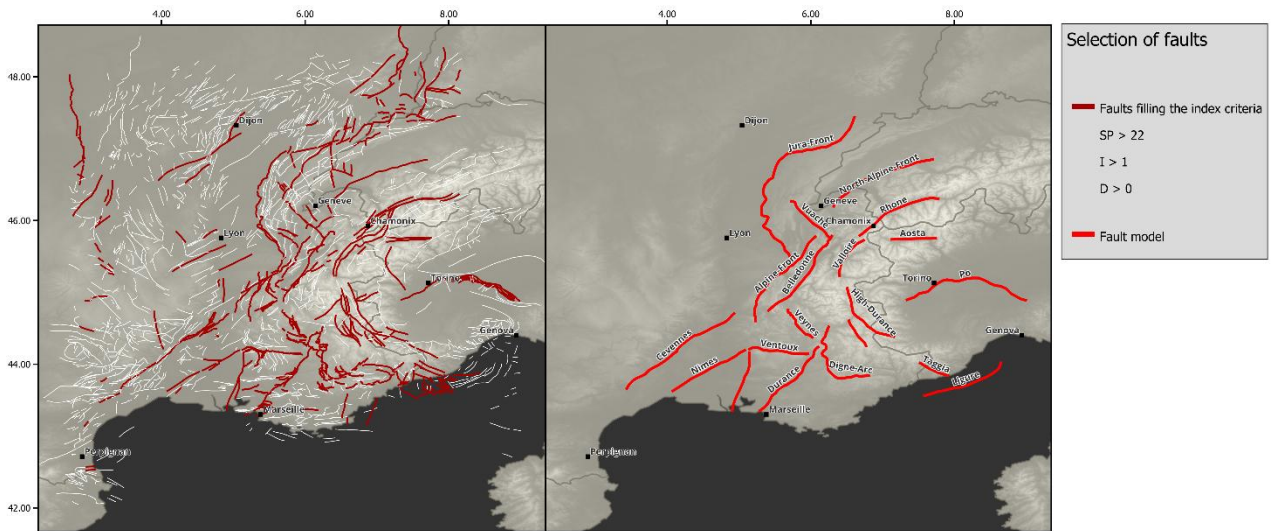
Figure 9

430   A) Selection of faults from SEFPAF filling the index criteria of Importance higher than 1, Documentation higher than 0, and
Seismogenic Potential higher than 22; B) Selected and idealized faults for a fault based seismic source model for PSHA.

Data type	Dataset	Reference	Nº of entities
Geological maps	French geological map	Chantraine et al., 2003	1819
	Italian geological map	Pantaloni, 2021	216
	Swiss geological map	swisstopo, 2024	30
Neotectonic fault datasets	BDFA	Jomard et al., 2017	136
	PACA-PO	Terrier et al., 2018	178
	Neotectonic map	Grellet et al., 1993	203
	ITHACA	Comerci et al., 2013	150
Regional studies	High Durance fault system	Sue and Tricart, 2003	27
	North Vuache fault system	Lallemand et al., 2024	16
	Belledonne fault system	Thouvenot et al., 2003	6
		Billant et al., 2015	2
	North Cevennes fault system	Thomasset et al., 2024	6
	Southern Alps active faults	Sanchez et al., 2010	23
	North alpine fault system	Bistacchi and Massironi, 2000	11
	Valais fault system	Champagnac et al., 2003	14
	Ligure fault system	Morelli et al., 2022	32
	Ubaye swarm fault	Jenatton et al., 2007	1
	Maurienne swarm fault	Guéguen et al., 2022	4
Neotectonic evidences	NEOPAL	Bertrand et al., 2007	37
	ASNR indexes	Baize et al., 2002	60

435   **Table 1**

Log gram of the input data used to compile SEFPAF, specifying the data type, the reference and the number of entities incorporated from each dataset in the compilation.

Mag bin	2 – 3	3 – 4	4 – 5	5 – 6	6 – 7
Time period	1975 – 2021	1820 – 2021	1800 – 2021	1750 – 2021	1350 – 2021

440

Table 2

Estimated completeness time periods per magnitude bin for the combined catalog FCAT (Manchuel et al., 2018) + BCSF Rénass (BCSF-Rénass, 2022). Magnitudes above Mw 2 are considered, although mainly events from Mw 3 and above have an actual impact on seismic flux values.

445

Fault_name	Length (km)	Strike (º)	Dip (º)	Direction (º)	Depth (km)	K	Slip (mm/y)	NeoT_age	I	D	SP	SP_n	SP_d	SP_s
Cevennes	170	40	65	130	10	N/SS-S	0.05	Historical	3	3	39	5	3	5
Nimes	103	45	65	135	10	R/SS-S		Holocene	3	3	43	4	3	3
Ventoux	68	90	45	180	10	R/SS-S	0.02	Holocene	3	3	27	4	2	3
Salon-Cavaillon	92	10	75	280	10	N/SS-D		Holocene	3	3	23	4	1	3
Durance	122	30	65	120	10	R/SS-S	0.1	Historical	3	3	45	5	2	6
Veynes	54	150	45	60	10	R/SS-D		Miocene	3	2	44	1	2	6
Digne-Arc	127	120	60	30	10	R/SS-D		Pleistocene	3	3	38	3	2	5
Ligure	104	55	45	325	10	R		Historical	3	2	50	5	2	7
Taggia	37	140	45	50	10	SS-D		Holocene	2	1	65	4	5	7
Po	155	90	45	180	10	R		Holocene	2	2	44	4	3	5
Parpaillon	43	160	80	250	10	N/SS-D		Holocene	3	3	49	4	3	6
High Durance	99	160	70	70	10	N		Holocene	3	2	54	2	5	7
Valloire	64	35	30	125	10	N			3	1	53	-1	5	5
Belledonne	138	30	80	120	10	R/SS-D		Holocene	3	3	43	4	4	5
Alpine-Front	153	20	40	110	10	R/SS-D	0.2	Pleistocene	3	3	43	3	3	5
Jura-Front	287	200	45	120	10	R/SS-S	0.2	Holocene	3	3	38	4	3	4
Vuache	73	140	80	50	10	SS-S		Historical	3	3	55	5	4	6
North-Alpine-Front	134	60	45	150	10	R		Miocene	2	2	32	1	3	3
Rhone	107	30	45	120	10	R/SS-D			3	1	48	-1	4	5
Aosta	47	90	80	0	10	SS		Holocene	3	1	48	4	4	3

Table 3

Database for the fault model with its corresponding parameters: Fault length and strike are estimated from the idealized fault trace; dip and dip direction are derived from SEFPAF data when known; depth is assumed equal across all faults, based on an idealized geometry; The kinematics (K), slip rate (Slip) and neotectonic age (NeoT_age) comes from SEFPAF when documented; I, D, SP, SP_n, SP_d, SP_s are the highest index and sub-index values coming from the SEFPAF faults for which each idealized fault is inspired from. Italic values are assumed, as they are not documented in SEFPAF.

455

References

Angrand, P., Mouthereau, F.: Evolution of the Alpine orogenic belts in the Western Mediterranean region as resolved by the kinematics of the Europe-Africa diffuse plate boundary. BSGF - Earth Sci. Bull. 192, 42. https://doi.org/10.1051/bsgf/2021031, 2021

Arthaud, F., Matte, Ph.: Les decrochements tardi-hercyniens du sud-ouest de l'europe. Geometrie et essai de reconstitution des conditions de la deformation. Tectonophysics 25, 139–171. https://doi.org/10.1016/0040-1951(75)90014-1, 1975

Baize, S., Cushing, M., Lemeille, F., Granier, T., Grellet, B., Carbon, D., Combes, P., Hibsch, C.: Inventaire des indices de rupture affectant le quaternaire. - En relation avec les grandes structures connues en Francs métropolitaine et dans les régions limitrophes, Mém. Soc. géol. Fr., 2002, N°175, 142 pages. Institut de Radioprotection et de Sûreté Nucléaire (IRSN). Fontenay aux Roses, 2002

Bard, P.-Y., Lebrun, B., Rédacteurs principaux: Propositions pour un nouveau zonage sismique de la France, Recommandations de la cellule "aléa sismique" au GEPP. 162 p., 2004

Basili, R., Valensise, G., Vannoli, P., Burrato, P., Fracassi, U., Mariano, S., Tiberti, M.M., Boschi, E.: The Database of Individual Seismogenic Sources (DISS), version 3: Summarizing 20 years of research on Italy's earthquake geology. Tectonophysics 453, 20–43. https://doi.org/10.1016/j.tecto.2007.04.014, 2008

BCSF-Rénass, Mendel, V.: Instrumental seismicity in mainland France (1962-2021). https://doi.org/10.25577/FV3F-SQ09, 2022

Bellahsen, N., Mouthereau, F., Boutoux, A., Bellanger, M., Lacombe, O., Jolivet, L., Rolland, Y.: Collision kinematics in the western external Alps: Kinematics of the Alpine collision. Tectonics 33, 1055–1088. https://doi.org/10.1002/2013tc003453, 2014

Bellier, O., Cushing, E.M., Sébrier, M.: Thirty years of paleoseismic research in metropolitan France. Comptes Rendus. Géoscience 353, 339–380. https://doi.org/10.5802/crgeos.102, 2022

Ben-Zion, Y., Sammis, C.G.: Characterization of Fault Zones. Pure appl. geophys. 160, 677–715. https://doi.org/10.1007/PL00012554, 2003

Bertrand, A., Sue, C.: Reconciling late faulting over the whole Alpine belt: from structural analysis to geochronological constrains. Swiss J Geosci 110, 565–580. https://doi.org/10.1007/s00015-017-0265-4, 2017

Bertrand, G., Bellier, O., Bollinger, L., Cushing, E., Durouchoux, C., Hollender, F., Meyer, B., Sabourault, P., Schlupp, A., Sébrier, M., Herniot, P.: NéoPal: Base de données nationale des déformations néotectoniques et des paléoséismes, 2007

Bilau, A., Rolland, Y., Schwartz, S., Godeau, N., Guihou, A., Deschamps, P., Brigaud, B., Noret, A., Dumont, T., Gautheron, C.: Extensional reactivation of the Penninic frontal thrust 3 Myr ago as evidenced by U–Pb dating on calcite in fault zone cataclasite. Solid Earth 12, 237–251. https://doi.org/10.5194/se-12-237-2021, 2021

Billant, J., Hippolyte, J.-C., Bellier, O.: Tectonic and geomorphic analysis of the Belledonne border fault and its extensions, Western Alps. Tectonophysics 659, 31–52. https://doi.org/10.1016/j.tecto.2015.07.025, 2015

Bistacchi, A., Massironi, M.: Post-nappe brittle tectonics and kinematic evolution of the north-western Alps: an integrated approach. Tectonophysics 327, 267–292. https://doi.org/10.1016/S0040-1951(00)00206-7, 2000

Blès, J.L., Sauret, B., Godefroy, P., Martin, C.: Contribution à l'étude des dangers d'installations industrielles à « risque spécial » de la région Rhônes-Alpes. Presented at the Rapport BRGM R33623 GEO-SGN92, coll. Lambert J., 1992

Boudon, J., Gamond, J.F., Gratier, J.P., Robert, J.P., Depardon, J.P., Gay, M., Ruhland, M.: L'arc alpin occidental: réorientation de structures primitivement E–W par glissement et étirement dans un systeme de compression global N–S. Eclog. Geol. Helv., 69, 2, p. 509-519, 1976

Champagnac, J.D., Sue, C., Delacou, B.: Brittle orogen-parallel extension in the internal zones of the Swiss Alps (South Valais). Eclogae Geologicae Helvetiae, 2003/96/1-14, 2003

Chantraine, J., Autran, A., Cavelier, C.: Carte géologique de la France (version numérique) à l'échelle du millionième, 2003

Comerci, A.M., Blumetti, A.M., Manna, P.D., Fiorenza, D., Guerrieri, L., Lucarini, M., Serva, L., Vittori, E.: ITHACA Project and Capable Faults in the Po Plain (Northern Italy). Ingegneria Sismica. Anno XXX – N. 1-2. 36-50, 2013

Delacou, B., Sue, C., Champagnac, J.-D., Burkhard, M.: Origin of the current stress field in the western/central Alps: role of gravitational re-equilibration constrained by numerical modelling. SP 243, 295–310. https://doi.org/10.1144/GSL.SP.2005.243.01.19, 2005

505 Delacou, B., Sue, C., Champagnac, J.-D., Burkhard, M.: Present-day geodynamics in the bend of the western and central Alps as constrained by earthquake analysis. Geophysical Journal International 158, 753–774. https://doi.org/10.1111/j.1365-246X.2004.02320.x, 2004

DISS Working Group: Database of Individual Seismogenic Sources (DISS), version 3.3.0: A compilation of potential sources for earthquakes larger than M 5.5 in Italy and surrounding areas. https://doi.org/10.13127/DISS3.3.0, 2021

510 Gratier, J.P., Ménard, G., Arpin, R.: Strain-displacement compatibility and restoration of the Chaînes Subalpines of the western Alps. Geological Society, London, Special Publications, 1989

Grellet, B., Combes, P., Granier, T., Philip, H.: Sismotectonique de la France métropolitaine dans son cadre géologique et géophysique: volume 1, Institut de Radioprotection et Sûreté nucléaires. ed. Mém. n. s. Soc. géol. Fr., no 164, 1993

Guéguen, P., Janex, G., Nomade, J., Langlais, M., Helmstetter, A., Coutant, O., Schwartz, S., Dollet, C.: Unprecedented
515 seismic swarm in the Maurienne valley (2017–2019) observed by the SISmalp Alpine seismic network: operational monitoring and management. Comptes Rendus. Géoscience 353, 517–534. https://doi.org/10.5802/crgeos.70, 2022

Haller, K.M., Basili, R.: Developing Seismogenic Source Models Based on Geologic Fault Data. Seismological Research Letters 82, 519–525. https://doi.org/10.1785/gssrl.82.4.519, 2011

Handy, M.R., M. Schmid, S., Bousquet, R., Kissling, E., Bernoulli, D.: Reconciling plate-tectonic reconstructions of Alpine
520 Tethys with the geological–geophysical record of spreading and subduction in the Alps. Earth-Science Reviews 102, 121–158. https://doi.org/10.1016/j.earscirev.2010.06.002, 2010

Hanks, T.C., Kanamori, H.: A moment magnitude scale. J. Geophys. Res. 84, 2348–2350. https://doi.org/10.1029/JB084iB05p02348, 1979

IAEA: Seismic Hazards in Site Evaluation for Nuclear Installations, Specific Safety Guide. International Atomic Energy
525 Agency, Vienna, 2010

Janjou, D.: Descriptif des cartes géologiques à 1/50 000 format "vecteurs", BRGM, Orléans, 2004

Jenatton, L., Guiguet, R., Thouvenot, F., Daix, N.: The 16,000-event 2003–2004 earthquake swarm in Ubaye (French Alps). J. Geophys. Res. 112, 2006JB004878. https://doi.org/10.1029/2006JB004878, 2007

Jomard, H., Cushing, E.M., Palumbo, L., Baize, S., David, C., Chartier, T.: Transposing an active fault database into a seismic
530 hazard fault model for nuclear facilities – Part 1: Building a database of potentially active faults (BDFA) for metropolitan France. Nat. Hazards Earth Syst. Sci. 17, 1573–1584. https://doi.org/10.5194/nhess-17-1573-2017, 2017

Lallemand, T., Quiquerez, A., Audin, L., Baize, S., Grebot, R., Mathey, M.: Combining geological and archaeological evidence to infer the recent tectonics of the Montagne du Vuache Fault, Jura Mountains, France. PAGES Mag 32, 16–17. https://doi.org/10.22498/pages.32.1.16, 2024

535 Larroque, C., Baize, S., Albaric, J., Jomard, H., Trévisan, J., Godano, M., Cushing, M., Deschamps, A., Sue, C., Delouis, B., Potin, B., Courboulex, F., Régnier, M., Rivet, D., Brunel, D., Chèze, J., Martin, X., Maron, C., Peix, F.: Seismotectonics of southeast France: from the Jura mountains to Corsica. Comptes Rendus. Géoscience 353, 105–151. https://doi.org/10.5802/crgeos.69, 2022

Le Pichon, X., Rangin, C.: Geodynamics of the France Southeast Basin: importance of gravity tectonics. Bulletin de la Société
540 Géologique de France 181, 476–476. https://doi.org/10.2113/gssgfbull.181.6.476, 2010

Leonard, M.: Self-Consistent Earthquake Fault-Scaling Relations: Update and Extension to Stable Continental Strike-Slip Faults. Bulletin of the Seismological Society of America 104, 2953–2965. https://doi.org/10.1785/0120140087, 2014

Machette, M.N.: Active, capable, and potentially active faults — a paleoseismic perspective. Journal of Geodynamics 29, 387–392. https://doi.org/10.1016/S0264-3707(99)00060-5, 2000

545 Malavieille, J.: Late Orogenic extension in mountain belts: Insights from the basin and range and the Late Paleozoic Variscan Belt. Tectonics 12, 1115–1130. https://doi.org/10.1029/93TC01129, 1993

Malavieille, J., Guihot, P., Costa, S., Lardeaux, J.M., Gardien, V.: Collapse of the thickened Variscan crust in the French Massif Central: Mont Pilat extensional shear zone and St. Etienne Late Carboniferous basin. Tectonophysics 177, 139–149. https://doi.org/10.1016/0040-1951(90)90278-G, 1990

550   Manatschal, G., Chenin, P., Haupert, I., Masini, E., Frasca, G., Decarlis, A.: The Importance of Rift Inheritance in Understanding the Early Collisional Evolution of the Western Alps. Geosciences 12, 434. https://doi.org/10.3390/geosciences12120434, 2022

Manchuel, K., Traversa, P., Baumont, D., Cara, M., Nayman, E., Durouchoux, C.: The French seismic CATalogue (FCAT-17). Bull Earthquake Eng 16, 2227–2251. https://doi.org/10.1007/s10518-017-0236-1, 2018

555   Masson, C., Mazzotti, S., Vernant, P., Doerflinger, E.: Extracting small deformation beyond individual station precision from dense Global Navigation Satellite System (GNSS) networks in France and western Europe. Solid Earth 10, 1905–1920. https://doi.org/10.5194/se-10-1905-2019, 2019

Mathey, M., Sue, C., Pagani, C., Baize, S., Walpersdorf, A., Bodin, T., Husson, L., Hannouz, E., Potin, B.: Present-day geodynamics of the Western Alps: new insights from earthquake mechanisms. Solid Earth 12, 1661–1681.
560   https://doi.org/10.5194/se-12-1661-2021, 2021

Matte, Ph., Burg, J.P.: Sutures, thrusts and nappes in the Variscan Arc of western Europe: plate tectonic implications. SP 9, 353–358. https://doi.org/10.1144/GSL.SP.1981.009.01.31, 1981

Matte, Ph., Mattauer, M.: Hercynian orogeny in the Pyrenees was not a rifting event. Nature 325, 739–740. https://doi.org/10.1038/325739b0, 1987

565   Ménard, G., Molnar, P.: Collapse of a Hercynian Tibetan Plateau into a late Palaeozoic European Basin and Range province. Nature 334, 235–237. https://doi.org/10.1038/334235a0, 1988

Michetti, A.M., Serva, L., Vittori, E.: ITHACA Italy Hazard from Capable Faults: a Database of Active Faults of the Italian Onshore Territory. CD-Rom and Explanatory Notes. ANPA, Rome, Italy, 2000

Mohn, G., Manatschal, G., Beltrando, M., Masini, E., Kusznir, N.: Necking of continental crust in magma-poor rifted margins:
570   Evidence from the fossil Alpine Tethys margins. Tectonics 31, 2011TC002961. https://doi.org/10.1029/2011TC002961, 2012

Morelli, D., Locatelli, M., Corradi, N., Cianfarra, P., Crispini, L., Federico, L., Migeon, S.: Morpho-Structural Setting of the Ligurian Sea: The Role of Structural Heritage and Neotectonic Inversion. JMSE 10, 1176. https://doi.org/10.3390/jmse10091176, 2022

575   Mowbray, V., Sue, C., Baize, S., Beauval, C., Mathey, M., Lemoine, A., Walpersdorf, A., & Granier, E.: South East France Potentially Active Faults [Data set]. Zenodo. https://doi.org/10.5281/zenodo.17235395, 2025

Muir Wood, R., Mallard, D.J.: When is a fault 'extinct'? JGS 149, 251–254. https://doi.org/10.1144/gsjgs.149.2.0251, 1992

Pantaloni, M.: The 1:1M geological map of Italy: a milestone in geological knowledge. Physis, 56(1-2), 383-396. https://doi.org/10.15161/oar.it/r1nfh-cq808, 2021

580   Piña-Valdés, J., Socquet, A., Beauval, C., Doin, M., D'Agostino, N., Shen, Z.: 3D GNSS Velocity Field Sheds Light on the Deformation Mechanisms in Europe: Effects of the Vertical Crustal Motion on the Distribution of Seismicity. JGR Solid Earth 127, e2021JB023451. https://doi.org/10.1029/2021JB023451, 2022

Ritz, J.-F.: Évolution du champ de contraintes dans les Alpes du Sud depuis la fin de l'Oligocène. Implications sismotectoniques. Tectonique. Thèse. Université Montpellier II - Sciences et Techniques du Languedoc, 187 p., 1991

585   Roure, F., Brun, J.-P., Colletta, B., Van Den Driessche, J.: Geometry and kinematics of extensional structures in the alpine foreland basin of southeastern France. Journal of Structural Geology 14, 503–519. https://doi.org/10.1016/0191-8141(92)90153-n, 1992

Sanchez, G., Rolland, Y., Schreiber, D., Giannerini, G., Corsini, M., Lardeaux, J.-M.: The active fault system of SW Alps. Journal of Geodynamics 49, 296–302. https://doi.org/10.1016/j.jog.2009.11.009, 2010

590   Sébrier, M., Ghafiri, A., Bles, J.-L.: Paleoseismicity in France: Fault trench studies in a region of moderate seismicity. Journal of Geodynamics 24, 207–217. https://doi.org/10.1016/s0264-3707(97)00005-7, 1997

Serpelloni, E., Cavaliere, A., Martelli, L., Pintori, F., Anderlini, L., Borghi, A., Randazzo, D., Bruni, S., Devoti, R., Perfetti, P., Cacciaguerra, S.: Surface Velocities and Strain-Rates in the Euro-Mediterranean Region from Massive GPS Data Processing. Front. Earth Sci. 10, 907897. https://doi.org/10.3389/feart.2022.907897, 2022

595   Share, P.-E., Táboŕík, P., Štěpančíková, P., Stemberk, J., Rockwell, T.K., Wade, A., Arrowsmith, J.R., Donnellan, A., Vernon, F.L., Ben-Zion, Y.: Characterizing the uppermost 100 m structure of the San Jacinto fault zone southeast of Anza, California, through joint analysis of geological, topographic, seismic and resistivity data. Geophysical Journal International 222, 781–794. https://doi.org/10.1093/gji/ggaa204, 2020

Shen, Z., Wang, M., Zeng, Y., Wang, F.: Optimal Interpolation of Spatially Discretized Geodetic Data. Bulletin of the Seismological Society of America 105, 2117–2127. https://doi.org/10.1785/0120140247, 2015

Slemmons, D. B., & McKinney, R.: Definition of 'active fault'. Final report. Department of the Army, Corps of Engineers, Waterways Experiment Station, Soils and Pavements Laboratory. ed., Vicksburg, MS (USA), 1977

Sue, C., Thouvenot, F., Fréchet, J., Tricart, P.: Widespread extension in the core of the western Alps revealed by earthquake analysis. J. Geophys. Res. 104, 25611–25622. https://doi.org/10.1029/1999JB900249, 1999

Sue, C., Tricart, P.: Neogene to ongoing normal faulting in the inner western Alps: A major evolution of the late alpine tectonics. Tectonics 22, 2002TC001426. https://doi.org/10.1029/2002TC001426, 2003

swisstopo: Tectonic Map of Switzerland 1: 500 000. – Federal Office of Topography swiss-topo, Wabern, 2024

Tapponnier, P.: Rigid-plastic indentation and tectonic evolution of the Alpine system in Europe. Int. Syrup. Structural History of the Mediterranean Basins. Ed. Technip., Paris, 1977

Terrier, M.: Identification et classification des failles actives de la Provence-Alpes-Côte d'Azur. Phase 2: Analyse et synthèse des connaissances actuelles sous la forme de fiches descriptives des failles. Rapport BRGM-RP-53151-FR, 2 volumes, 350 p., 2004

Terrier, M.: Néotectonique de la Provence occidentale (France): vers une analyse multicritères des déformations récentes. Application à la classification des structures sismogènes. Thèse de l'université de Provence, Document du BRGM, 207, 232 p., 1991

Terrier, M., Bertil, D., Rohmer, J.: Méthode d'identification des failles actives en domaine de déformation lente. Rapport final. Rapport BRGM/RP-68 553-FR, p.87, fig.18, tabl. 5, ann. 2, 2018

Thomasset, C., Ritz, J.-F., Pouliquen, S., Manchuel, K., Le-Roux-Mallouf, R.: Geometry and tectonic history of the Northeastern Cévennes Fault System (Southeast Basin, France): new insights from deep seismic reflection profiles. BSGF - Earth Sci. Bull. 195, 17. https://doi.org/10.1051/bsgf/2024016, 2024

Thouvenot, F., Fréchet, J., Jenatton, L., Gamond, J.-F.: The Belledonne Border Fault: identification of an active seismic strike-slip fault in the western Alps. Geophysical Journal International 155, 174–192. https://doi.org/10.1046/j.1365-246X.2003.02033.x, 2003

Valla, P.G., Sternai, P., Fox, M.: How Climate, Uplift and Erosion Shaped the Alpine Topography. Elements 17, 41–46. https://doi.org/10.2138/gselements.17.1.41, 2021

Walpersdorf, A., Pinget, L., Vernant, P., Sue, C., Deprez, A., the RENAG team: Does Long-Term GPS in the Western Alps Finally Confirm Earthquake Mechanisms? Tectonics 37, 3721–3737. https://doi.org/10.1029/2018TC005054, 2018

Walpersdorf, A., Sue, C., Baize, S., Cotte, N., Bascou, P., Beauval, C., Collard, P., Daniel, G., Dyer, H., Grasso, J.-R., Hautecoeur, O., Helmstetter, A., Hok, S., Langlais, M., Menard, G., Mousavi, Z., Ponton, F., Rizza, M., Rolland, L., Souami, D., Thirard, L., Vaudey, P., Voisin, C., Martinod, J.: Coherence between geodetic and seismic deformation in a context of slow tectonic activity (SW Alps, France). Journal of Geodynamics 85, 58–65. https://doi.org/10.1016/j.jog.2015.02.001, 2015

Wu, Z., Hu, M.: Definitions, Classification Schemes for Active Faults, and Their Application. Geosciences 14, 68. https://doi.org/10.3390/geosciences14030068, 2024